# Instrument for measurement of singlet oxygen for studies of skin under UVA irradiation

S. J. Davis[a], D. I. Rosen[a], J. England[a], M. F. Hinds[a], R. K. Sivamani[b], and W. Burney[b]
[a]Physical Sciences Inc., 20 New England Business Center, Andover, MA USA 01810-1077
[b]University of California, Davis, Department of Dermatology, 3301 C Street, Suite 1400, Sacramento, CA USA 95816-3367

## ABSTRACT

In this paper we will describe a non-intrusive, optically-based instrument that can quantitatively measure singlet molecular oxygen, a constituent of reactive oxygen species (ROS) produced by irradiation of human skin by the longer wavelength UV radiation known as UVA. UVA is causally associated with DNA damage and subsequent development of melanoma. We will present data from healthy human subjects that show formation of singlet molecular oxygen and concomitant production of thymine dimers, indicative of DNA damage. We will also discuss how this instrument may be a valuable tool for the development of more effective sunblock formulations for UVA.

**Keywords:** Skin damage, reactive oxygen species, singlet oxygen, ultraviolet solar radiation

## 1. INTRODUCTION

Ultraviolet radiation (UV) is a known skin carcinogen[1-4] and generates reactive oxygen species (ROS) in the skin.[1-4] The UV spectrum that bypasses the atmospheric ozone layer includes two subsets, UVA and UVB, where UVA radiation is further divided into UVA1 and UVA2 (Table 1). Both UVA and UVB are classified as Class I carcinogens by the International Agency for Research on Cancer.[1] There is causal evidence that UVB induces mutations causing non-melanoma skin cancers.[5-7] In addition there is strong evidence that UVA exposure may lead to melanoma.[4-9] Current sunscreen product labeling guidelines require information regarding protection against both UVB and UVA.[10] *In vivo* sunscreen testing against erythemogenic wavelengths (UVB and UVA2) involves evaluation of the sun protection factor (SPF). A complete assessment including UVA and UVB radiation requires a non-invasive *in vivo* measurement of the effects of UVA1 exposure. Sunscreens are currently only tested for protection against UVA through *in vitro* measurements.[10] As ultraviolet radiation from sunlight is predominantly composed of UVA (twenty times higher intensity than UVB), the *in vitro* measurements are insufficient for quantitative characterization of sunscreen products for UVA, especially for UVA1 and even longer wavelength, visible solar radiation which also produces DNA damage.[11,12]

**Table 1.** Ultraviolet Radiation Bands

| Band | Wavelength Range | Non-Invasive In Vivo Measures |
|---|---|---|
| UVA1 | 340 – 400 nm | None |
| UVA2 | 320 – 340 nm | Sun Protection Factor |
| UVB | 280 – 320 nm | Sun Protection Factor |

Each year in the U.S. alone over 5.4 million cases of nonmelanoma skin cancer are treated in more than 3.3 million people.[13] The annual cost of treating skin cancers in the U.S. is estimated at $8.1 billion: about $4.8 billion for nonmelanoma skin cancers and $3.3 billion for melanoma.[14]

UVA1 radiation can induce the production of multiple reactive oxygen species (ROS): $O_2(a)$, $H_2O_2$, and $O_2^-$.[4,11,12] Among these species, singlet oxygen ($O_2(a)$) can be non-invasively measured through detection of its luminescence at 1270 nm.[15-19,20,21] UVA1 is especially concerning because it can penetrate skin deeper and cause DNA damage.[4] There is also direct evidence that visible wavelength light also produces ROS, proinflammatory cytokines, and matrix metaloproteinase expression.[22,23] Although both UVA and UVB can generate ROS, no broadly accepted *in vivo* assessments against UVA1 exposure are currently used. Therefore, an *in vivo* test that allows for the measurement of

*sjd@psicorp.com; phone 1 978 689-0003; fax 1 978 689-3232; psicorp.com

UVA1 generated singlet oxygen would serve as an important quantitative advance for human testing and the development of more protective sunscreens. Although the SPF does not measure all of the effects of UVB or UVA2, it measures erythema, a reproducible effect *in vivo* that has enabled use in quantifying sunscreen protection. It is now well recognized that UVA damages skin either by direct DNA absorption or by an oxygen dependent photodynamic process and is implicated in skin cancer development as well as photo-aging.[4] Direct absorption of UVA can lead to dimerization of pyrimidine bases and the oxygen dependent photodynamic process leads to lesions such as 8-oxoquanine (8-oxyGua).

# 2. APPROACH

## *2.1* Background

Optical detection of the weak singlet oxygen emission signal is challenging due to the presence of multiple species emitting light at overlapping wavelengths. The fundamental photodynamic UVA excitation process for singlet oxygen via tissue irradiation is illustrated in Figure 1. Endogenous photosensitizers (PS) such as porphyrins in skin absorb the UVA, promoting them to the first excited singlet state ($S_1$), from which strong radiation to the ground singlet state produces visible through near IR fluorescence at wavelengths characteristic of the PS. The excited singlet state also has a large probability of intrasystem crossing to the triplet state ($T_1$), which is nearly resonant with the transition of oxygen from ground state ($^3\Sigma$) to excited singlet state ($^1\Delta$). Collisions between this metastable PS molecule and ground state oxygen that is present in skin populate the singlet delta state of oxygen which has an energy of 0.8 electron volts and emits in a narrow (~20 nm-wide) near-infrared (NIR) band at 1270 nm. Unfortunately, compared to other NIR emissions, singlet oxygen luminescence is very weak because of a long radiative lifetime and strong quenching, particularly in aqueous and protein-laden *in vivo* media such as skin. Furthermore, the PS produces strong $S_1$ fluorescence and extended fluorescence background from $T_1$. This process, known as the Type II PDT mechanism[4] is active when skin is exposed to UVA. Several endogenous photosensitizers absorb the UVA radiation and this initiates the process shown in Figure 1. These endogenous photosensitizers include: flavins, urocanic acid, and some sterols.[4,20]

The major technical challenge for an *in vivo* optical monitor for singlet oxygen is the extraction of the singlet oxygen luminescence from these interferences. We have previously developed and demonstrated solutions to this challenge.[15-19] For the UVA on skin application we use spectral discrimination. This involves isolating the weak singlet oxygen emission centered at 1270 nm from other background emission sources such as broadband PS fluorescence and phosphorescence, and tissue autofluorescence while the irradiation light source is on. Figure 2 shows a depiction of a typical, near-IR optical emission spectrum. The monotonically decreasing curve is due to the prompt (10 ns lifetime) fluorescence spectrum from the PS. In this study we used a VariSpec liquid crystal tunable filter (LCTF) to sample several wavelengths that contained the singlet oxygen feature. This device, with no moving parts, is an electronically tunable transmission spectrometer allowing completely resolved spectra to be recorded. We used this device to monitor the entire singlet oxygen spectrum even in the presence of strong PS background fluorescence. The LCTF had an instrumental linewidth of ~ 20 nm, ideal for the singlet oxygen luminescence linewidth, also ~20 nm. By measuring the PS background at multiple wavelengths afforded by the LCTF operation, the true PS baseline can be quite sensitively and precisely defined and subtracted to allow ultra-sensitive detection of the singlet oxygen produced by relevant solar UVA levels of irradiation.

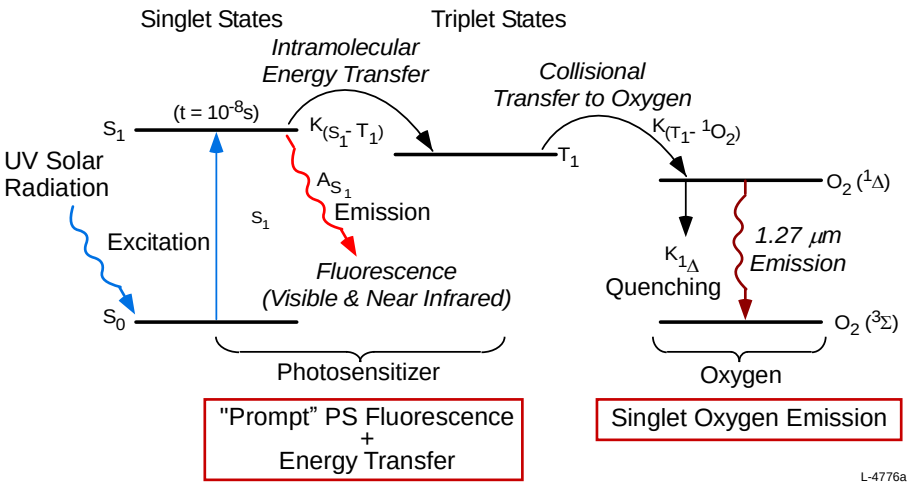


**Figure 1.** Photodynamic production of singlet oxygen in skin.

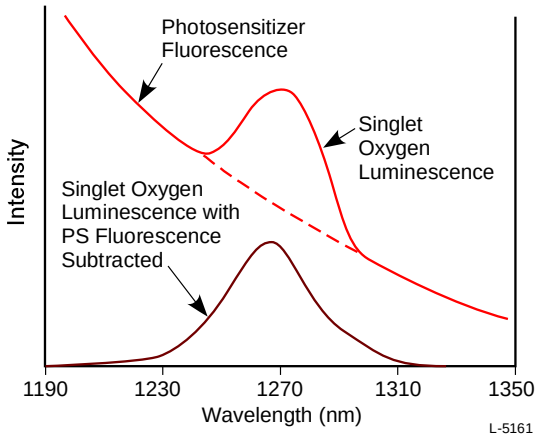


**Figure 2.** Strategy for separating the singlet oxygen near IR emission from the background photosensitizer fluorescence.

### 2.2 System Description

#### 2.2.1 UVA Light Source

We used a commercial, fiber optic coupled Hg lamp-based UV light source. The distal end of the fiber optic coupled UVA1 light source emitted over 100 mW of output between 350 and 400 nm with the peak intensity at ~350 nm. A pair of UVA transmission filters were used at the distal end of the fiber to ensure that the output was in the UVA region.

We used a long pass dichroic filter (turn on at 350 nm) to produce only UVA1 output from 350 to 400 nm. This configuration produced only UVA1 (no UVB). We also used a set of calibrated neutral density filters that readily attached to the distal end of the fiber bundle to reproducibly vary the UVA1 output to power levels from 1 to 80 mW.

#### 2.2.2 Detection Method and System

The singlet $O_2$ emission at 1.27 μm is from a very weak transition. In this wavelength region, there are also other emission sources besides the singlet $O_2$ emission, such as broadband photosensitizer (PS) fluorescence and phosphorescence, optical component emission, and tissue autofluorescence. The detection of the near-IR light produced by UVA1 irradiated skin was enabled by an ultra-sensitive Series 10330 photomultiplier tube (PMT) manufactured by Hamamatsu. A 3 mm diameter liquid light guide (LLG) collected the near-IR emission and carried this optical radiation to a collimation lens before it was incident on the LCTF. The light transmitted by the LCTF was focused onto the photocathode of the PMT. The photoelectrons produced by the PMT were counted using a photon counter board in the PC that controlled the entire singlet oxygen dosimeter.

The peak of the singlet oxygen emission feature occurs at 1270. The spectrum in tissue is ~20 nm wide, and the bandwidth of the LCTF is also ~20 nm. The convolution of these two Gaussian lineshapes results in an observed bandwidth of ~30 nm. As we describe below we used the seven wavelengths shown in Table 2.

**Table 2.** Wavelengths used to Measure Singlet Oxygen Emission

| Wavelength (nm) |
|---|
| 1230 |
| 1250 |
| 1260 |
| 1270 |
| 1280 |
| 1290 |
| 1310 |

A block diagram of the major components of the lab prototype singlet oxygen sensor is shown in Figure 3. Figure 4 is a photo of the UVA lamp, fiber bundle, and a light box to reduce ambient light while measurements are being recorded.

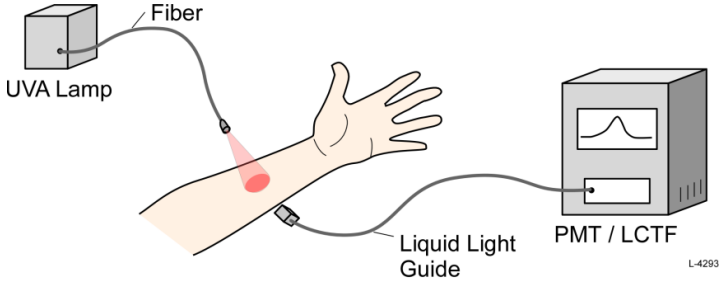


- Liquid crystal tunable filter tunes across O2 (a→X) system
- PMT in photon counting mode

**Figure 3.** Block diagram of the singlet oxygen monitor.

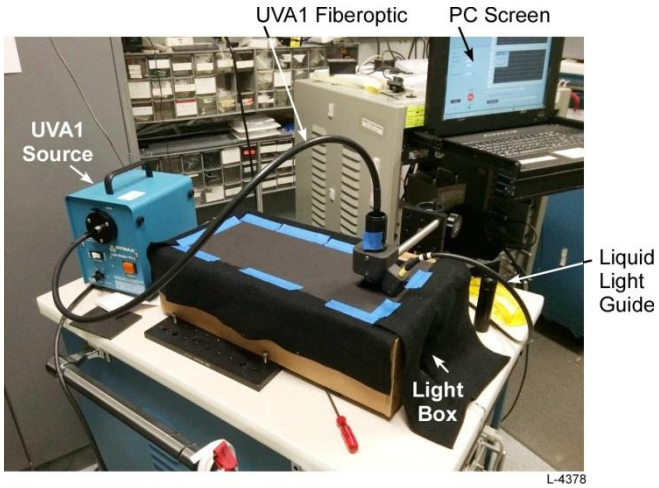


**Figure 4.** Photo of system prior to delivery to UCD.

The UVA light fiber was mounted in an adjustable, stable holder as shown in Figure 4. We also included a background minimization box that reduces ambient light to acceptable levels. As described above, the intensity is selected using a series of ND filters. The typical size of the illumination spot was ~ 2 cm diameter. The intensity incident on the skin was systematically varied from 0.4 to 25 mW/cm$^2$ and from 0.4 to 17.5 mW/cm$^2$ for the *ex-vivo* and *in-vivo* studies respectively.

The output of the photon counter was displayed on the PC screen including: raw photon counts, background, and background subtracted counts. The background subtracted counts for the seven wavelengths used are also displayed in real time on the PC screen along with a Gaussian fit to the singlet oxygen spectrum. The screen also displays the sum of the counts in each of the in-band wavelengths and the standard deviation in the sum. Since the data were recorded at these seven wavelengths, this sum is the best representation of the relative singlet oxygen measured in the run. This is summarized in Figure 5.

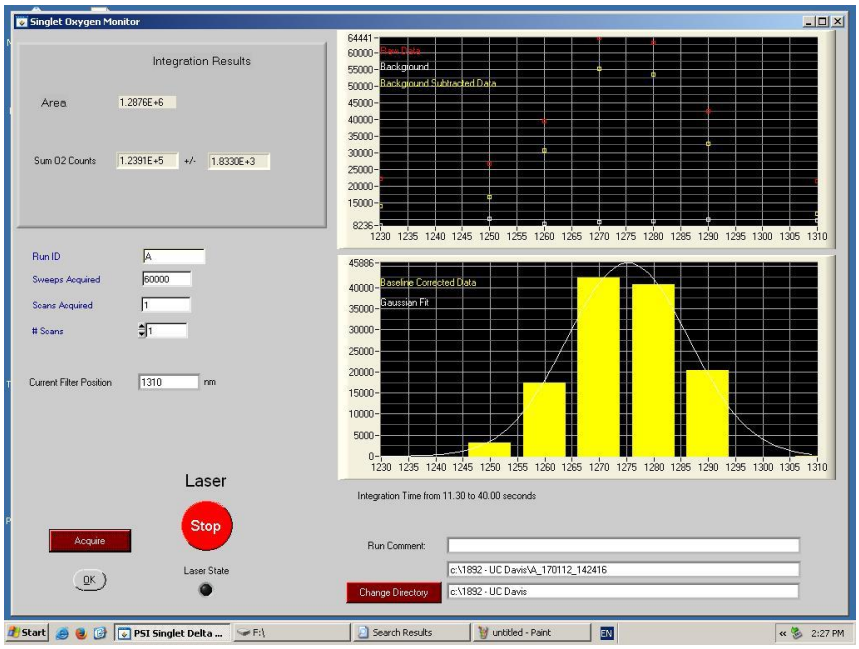


**Figure 5.** Data acquisition screen. See text for explanation.

We completed preliminary *in-vitro* tests using the photosensitizer benzoporphyrin derivative (BPD). It is an efficient producer of singlet oxygen by the Type II process illustrated in Figure 1 above. We used mixtures of BPD in both methanol and water in 1cm x 1cm square cuvettes over a range of BPD concentrations (1-20 uM). Initially, we operated the LCTF over many wavelengths to better understand the characteristics of the PS and singlet oxygen emission excited by UVA1. A typical spectrum is shown in Figure 6. These data clearly show the broadband PS fluorescence and the singlet oxygen feature. It is important to note that in methanol, the singlet oxygen is only mildly quenched, so that it appears to be a very strong signal. However, in tissue the singlet oxygen is much more severely quenched due to collisions with surrounding tissue. Indeed, it is these collisions that cause the tissue damage as the excited singlet oxygen releases nearly one electron volt per quenching event.

By subtracting the baseline emission from the total signal, we obtain the singlet oxygen luminescence spectrum show at the bottom of Figure 6. Note that in the Phase I system, the data recording, subtraction of the background, and fit to a Gaussian function are completed in real time using custom software developed for this program. This provides the user with a quantitative determination of the relative singlet oxygen concentration immediately after each measurement.

We systematically varied the UVA1 intensity with the ND filters and observed that the singlet oxygen signal changed linearly as the UVA1 intensity was varied over a range two orders of magnitude. We also confirmed that the spectral signal was indeed due to singlet oxygen, by bubbling gaseous nitrogen through the cuvette and observing that the spectral feature was reduced by over 90%. When the nitrogen flow was turned off, the signal rapidly returned as atmospheric oxygen returned to its equilibrium concentration in the methanol as expected by Henry's Law.

The system was calibrated using a black body radiation source to measure absolute response. In brief, the Liquid Light Guide (LLG) viewed the black body and the irradiance was recorded at several wavelengths including 1.275 μm, the center of the singlet oxygen feature. From this absolute source, we calculated that the entire system had a response of one photoelectron count from the photon counter for every 1200 photons collected by the LLG.

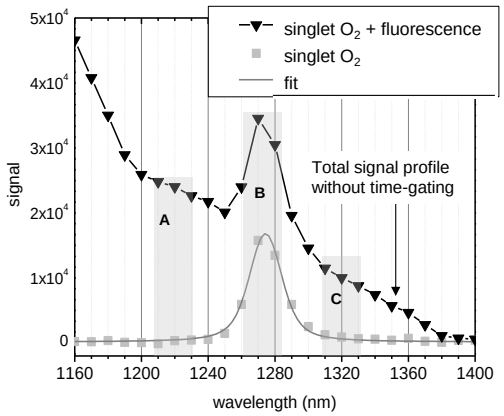


**Figure 6.** Typical spectra for PS fluorescence and singlet oxygen emission. The top trace shows the broad continuum background emission and the singlet oxygen spectral feature centered at 1.275 μm. The bottom trace shows the singlet oxygen spectrum after the background has been subtracted.

In order to describe the nature of the near-IR signals observed for both the *ex-vivo* and *in-vivo* studies we present Figure 7 that shows a typical recording of a run on the volar forearm of a healthy human. The UVA1 beam diameter was 2 cm and the total fluence was 432 mJ/cm$^2$ (10 mW/cm$^2$ delivered over a 42 second period).The left panel shows strong near-IR background emission and the singlet oxygen spectrum subsequent to subtraction of this background. The right panel shows the seven recorded wavelengths on an expanded scale and a Gaussian fit to the data. Data similar to these were recorded for all *in-vivo* and *ex-vivo* studies. The singlet oxygen produced was measured by summing readings at the five central wavelengths. The automated data reduction software provided this value and a standard deviation of the five points from the Gaussian fit.

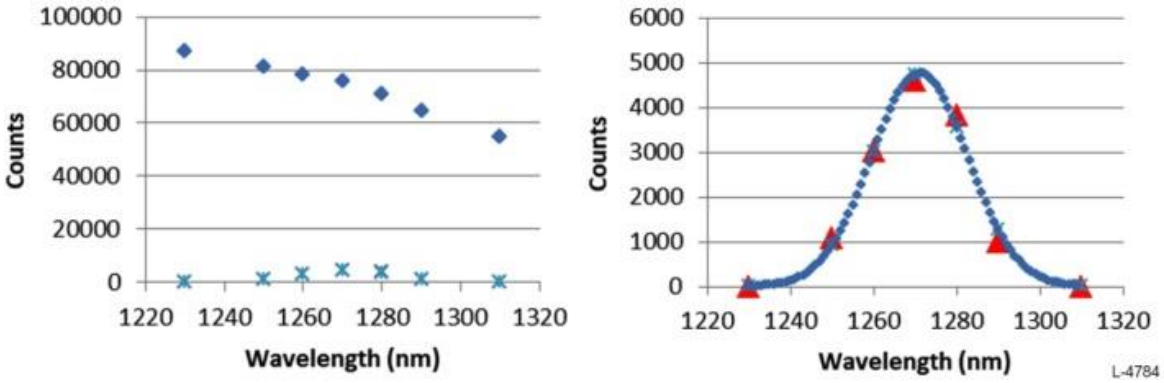


**Figure 7.** CW detection of singlet oxygen from UVA1 illuminated human skin from a healthy human subject. Left panel: raw data and background subtracted. Right panel: Expanded scale of left panel data and Gaussian fit showing singlet oxygen luminescence spectrum.

## 3. *EX-VIVO* AND *IN-VIVO* STUDIES

### 3.1 UVA Ex Vivo Experiments.

The ex-vivo skin samples were obtained from the abdomen of healthy volunteers undergoing abdominoplasties through the Plastic Surgery department at UC Davis Medical Center. This collection protocol was approved by the UC Davis Institutional Review Board. All of the skin samples were relatively sun-protected. The abdominal skin was cut into similar 2x2 cm pieces prior to experimentation with UVA1. After cleaning, they were rinsed twice in sterile PBS and excess subcutaneous fat was removed. All pieces were similar in size and shape and randomly assigned into the treatment groups. The samples from each set were labeled and treated with increasing doses of UVA1. Singlet oxygen counts were recorded for each fluence level (systematically varied with the ND filters described earlier). From these measurements, we observed a dose response of the singlet oxygen compared to the UVA1 exposure (Figure 8). UVA1

exposure was measured through the development of thymine dimers on histological analysis and the % thymine dimer expression was quantified on histological sections.

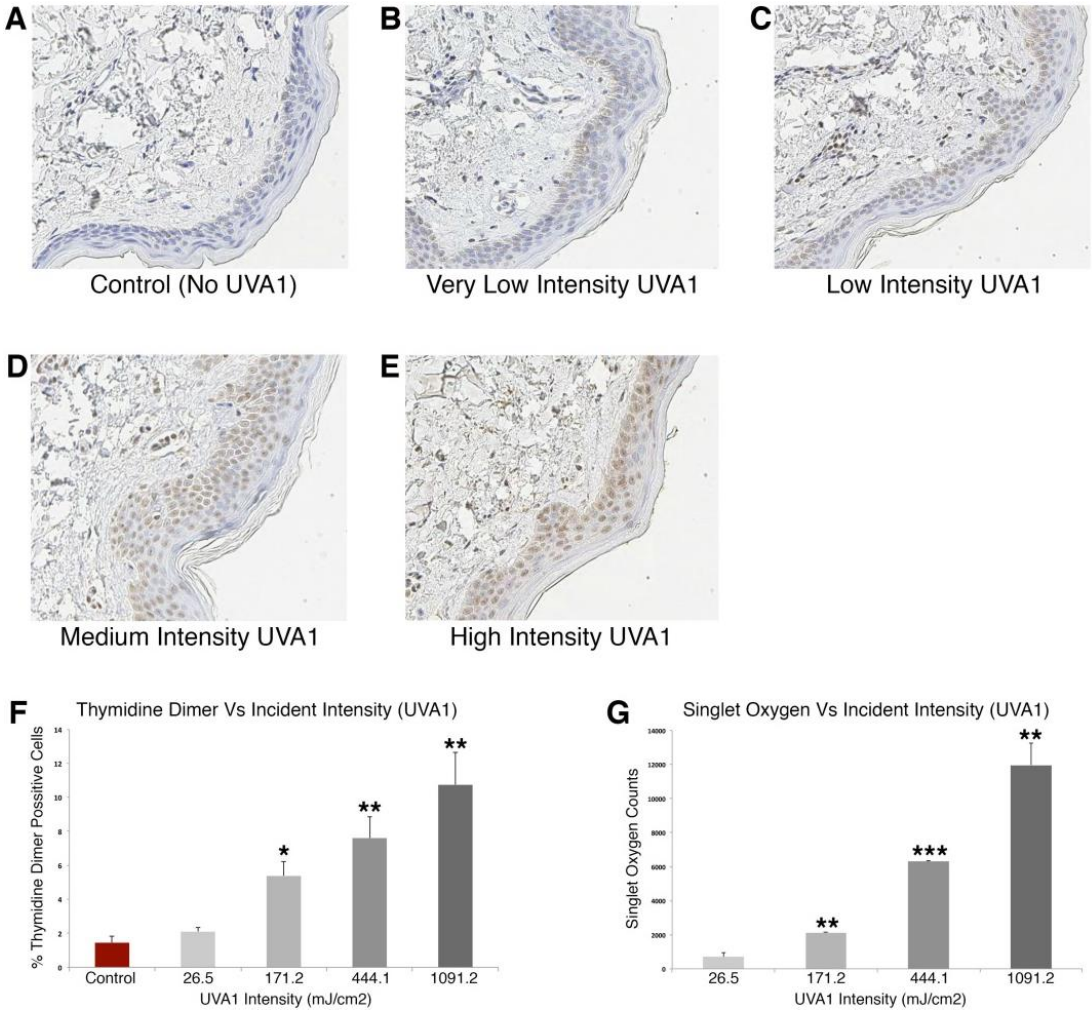


**Figure 8.** Increasing doses of UVA1 exposure of ex vivo human skin leads to increased expression of thymine dimers (A-F) and to increasing amounts of singlet oxygen(G). n=5 in each group.

### 3.2 In Vivo Experimentss.

Subjects were recruited from UC Davis and stratified based on their Fitzpatrick skin type into three groups (I/II, III/IV, and V/VI) and then their volar forearms were irradiated with UVA to assess singlet oxygen generation. All subjects provided written informed consent and the protocol was approved by the UC Davis Institutional Review Board. All subjects were exposed to dose escalations of UVA1 and higher Fitzpatrick skin types[24,25] were found to produce higher amounts of singlet oxygen (Figure 9). Melanin is an important factor in the reaction of skin to solar UVA radiation.[4,26-29]

We point out that the thymine dimer is produced by direct UVA1 damage to DNA. Thus, analysis for this product does not confirm that the singlet oxygen is doing the damage. In future work we will use an alternate product such as 8-oxo-7,8-dihydroguanine (8-oxo-Gua) as this represents reactive oxygen species related damage to the keratinocytes[30].

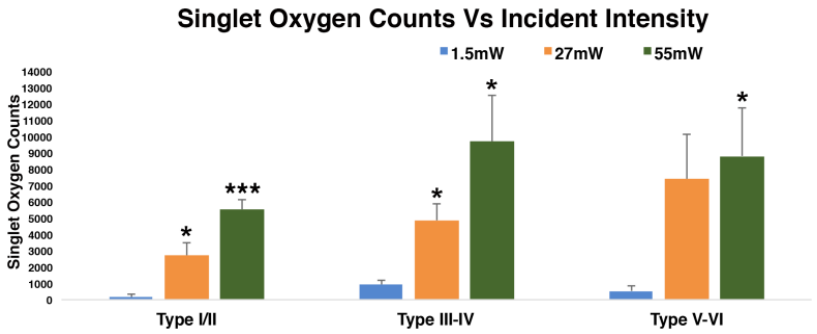


**Figure 9.** Singlet oxygen increases as UVA exposure is increased and with higher Fitzpatrick skin types.

We also completed a short study with two sunscreen formulations. This was conducted by applying sunscreens 15 minutes prior to UVA1 irradiation with either sunscreen or no sunscreen (control). Zinc oxide SPF 30 or avobenzone SPF 30 sunscreens were applied at 2 mg/cm$^2$. Based on dose response measures, a UVA1 fluence of 735 mJ/cm$^2$ was selected for sunscreen exposure studies. The preliminary observations were a) the avobenzone provided no measureable decrease in singlet oxygen production with respect to the control (no-sunscreen) and b) the Zinc oxide based sunscreen was found to increase the singlet oxygen production by up to a factor of five. While ZnO provides strong absorption for UVB and UVA, it is a strong photosensitizer under UVB and UVA irradiation and is a prodigious generator of singlet oxygen[31]. Whether this enhanced production is at the surface of the ZnO on the skin or can occur within depth is unknown and will be the subject of future studies.

## 4. SUMMARY AND CONCLUSIONS

We have successfully demonstrated that our optically-based, non-intrusive monitor can measure singlet oxygen produced by UVA1 illumination of human skin in real-time. We performed a systematic series of *ex-vivo* and *in-vivo* studies that showed that the singlet oxygen production increased monotonically as the UVA1 fluence was increased. We also completed histological examinations of skin *ex-vivo* that revealed a similar dependence for thymine dimer production with the UVA1 fluence.

Overall, the *ex vivo* and *in vivo* studies showed the following:

1) Singlet oxygen is reproducibly measurable in human skin (*ex vivo and in vivo*) as shown with dose escalation. Thymine dimer measurements *ex vivo* confirmed that the skin was irradiated with UVA at biological significant levels.
2) Increasing skin melanin leads to an increased generation of singlet oxygen
3) Zinc oxide in sunscreens leads to an increased generation of singlet oxygen

We believe that these results lay the foundation for further instrument development and testing to improve the understanding of skin damage from singlet oxygen and its relationship to skin cancer. We also believe that this same instrument could serve as a valuable tool for the development and *in-vivo* performance characterization of improved sunscreens for UVA protection.

## 5. REFERENCES

[1] F. El Ghissassi, R. Baan, K. Straif, Y. Grosse and B. Secretan, et al. (2009) A review of human carcinogens--part D: radiation. Lancet Oncol 10: 751-752.

[2] T. G. Polefka, T. A. Meyer, P. P. Agin and R. J. Bianchini (2012) Effects of solar radiation on the skin. J Cosmet Dermatol 11: 134-143.

[3] N. S. Agar, G. M. Halliday, R. S. Barnetson, H. N. Ananthaswamy, M. Wheeler, et al. (2004) The basal layer in human squamous tumors harbors more UVA than UVB fingerprint mutations: a role for UVA in human skin carcinogenesis. Proc Natl Acad Sci U S A 101: 4954-4959.

[4] J. Cadet and T. Douki, "Formation of UV-induced DNA damage contributing to skin cancer development," Photochemical & Photobiological Sciences, January 2018. DOI: 10.1039/c7pp00395a

[5] T. B. Buckel, A. M. Goldstein, M. C. Fraser, B. Rogers and M. A. Tucker, "Recent tanning bed use: a risk factor for melanoma," Arch. Dermatol., 2006, 142, 485-488.
[6] F. R. de Gruijl and H. Rebel, "Early events in UV carcinogenesis – DNA damage, target cells and mutant p53 foci," Photochem. Photobiol., 2008, 84, 382-387.
[7] K. H. Kraemer, "Sunlight and skin cancer: another link revealed," Proc. Natl. Acad. Sci. U.S.A., 1997, 94, 11-14.
[8] J. Reichrath and K. Rass, "Ultraviolet damage, DNA repair and vitamin D in nonmelanoma skin cencer and in malignant melanoma: an update," Adv. Exp. Med. Biol., 2014, 810, 208-233.
[9] A. Sample and Y. Y. He, "Mechanisms and prevention of UV-induced melanoma," Photodermatol., Photoimmunol. Photomed., 2018, 34, 13-24.
[10] Food and Drug Administration. Labeling and Effectiveness Testing; Sunscreen Drug Products for Over-the-Counter Human Use. Available at: http://www.gpo.gov/fdsys/pkg/FR-2011-06-17/pdf/2011-14766.pdf. Accessed March 28, 2014.
[11] L. Zastrow, N. Groth, F. Klein, D. Kockott, J. Lademann, R. Renneberg and L. Ferrero, "The Missing Link – Light-Induced (280-1,600 nm) Free Radical Formation in Human Skin," Skin Pharmacol Physiol 2009;22:31-44. DOI: 10.1159/000188083
[12] D. E. Godar (1999) UVA1 radiation triggers two different final apoptotic pathways. J Invest Dermatol 112: 3-12.
[13] http://www.skincancer.org/skin-cancer-information/skin-cancer-facts#general
[14] http://www.strategyr.com/MarketResearch/Sun_Care_Products_Market_Trends.asp
[15] S. Lee, L. Zhu, A. M. Minhaj, M. F. Hinds, D. H. Vu, D. I. Rosen, S. J. Davis and T. Hasan, "Pulsed Diode Laser-Based Monitor for Singlet Molecular Oxygen," J. Biomed. Opt. 13(3), 034010 (2008).
[16] H. J. Laubach, S. K. Chang, S. Lee, I. Rizvi, D. Zurakowski, S. J. Davis, C. R. Taylor and T. Hasan, "In vivo singlet oxygen dosimetry of clinical 5-aminolevulenic acid photodynamic therapy," J. Biomed. Opt. 13, 050504 (2008).
[17] S. Lee, D. H. Vu, M. F. Hinds, A. Liang, T. Hasan and S. J. Davis, "Pulsed Diode Laser-Based Singlet Oxygen Monitor for Photodynamic Therapy: in-vivo Studies of Tumor Laden Rats," J. Biomed. Opt. 13(6), 064035 (2008).
[18] S. Lee, M. E. Isabelle, K. L. Galbally-Kinney, B. W. Pogue and S. J. Davis, "Dual-channel imaging system for singlet oxygen and photosensitizer for PDT," Biomed. Opt. Express, 2(5), 1233-1242 (2011).
[19] S. Mallidi, S. Anbil, S. Lee, D. Manstein, S. Elrington, G. Kositratna, D. Schoenfeld, B. Pogue, S. J. Davis and T. Hasan, "Photosensitizer fluorescence and singlet oxygen luminescence as dosimetric predictors of topical 5-aminolevulinic acid photodynamic therapy induced clinical erythema," J. Biomed. Opt. 19(2), 028001 (February 06, 2014); doi: 10.1117/1.JBO.19.2.028001.
[20] J. Baier, T. Maisch, M. Maier, M. Landthaler and W. Baumler (2007) Direct detection of singlet oxygen generated by UVA irradiation in human cells and skin. J Invest Dermatol 127: 1498-1506.
[21] W. Baumler, J. Regensburger, A. Knak, A. Felgentrager and T. Maisch (2012) UVA and endogenous photosensitizers - the detection of singlet oxygen by its luminescence. Photochemical & Photobiological Sciences 11: 107-117.
[22] C. Marionnet, C. Pierrard, C. Golebiewski and F. Bernerd, Diversity of Biological Effects Induced by Longwave UVA Rays (UVA1) in Reconstructed Skin. PLoS ONE 9(8): e105263. Doi:10.1371/journal.pone.0105263.
[23] F. Liebel, S. Kaur, E. Ruvolo, N. Kollias and M. D. Southall, Irradiation of Skin with Visible Light Induces Reactive Oxygen Species and Matrix-Degrading Enzymes. Journal of Investigative Dermatology 132.7 (2012): 1901-1907.
[24] H. Lu, C. Edwards, S. Gaskell, A. Pearse and R. Marks(1996) Melanin content and distribution in the surface corneocyte with skin phototypes. Br J Dermatol 135: 263-267.
[25] M. Baquié and B. Kasraee (2013) Discrimination between cutaneous pigmentation and erythema: Comparison of the skin colorimeters Dermacatch and Mexameter. Skin Research and Technology: n/a-n/a.
[26] S. Premi, S. Wallisch, C. M. Mano, A. B. Weiner, A. Bacchiocchi, K. Wakamatsu, E. J. H. Bechara, R. Halaban. T. Douki and D. E. Brash, "Chemiexcitation of melanin derivatives induces DNA photoproducts long after UV exposure," Science, Vol. 347, Issue 6224, 20 February 2015.
[27] T. Kondo and V. J. Hearing (2011) Update on the regulation of mammalian melanocyte function and skin pigmentation. Expert Rev Dermatol 6: 97-108.
[28] M. Brenner and V. J. Hearing (2008) The protective role of melanin against UV damage in human skin. Photochem Photobiol 84: 539-549.
[29] S. Premi, S. Wallisch, C. M. Mano, A. B. Weiner, A. Bacchiocchi, K. Wakamatsu, E. J. H. Bechara, R. Halaban, T. Douki and D. E. Brash, "Chemiexcitation of melanin derivatives induces DNA photoproducts long after UV exposure," Science, Vol. 347, Issue 6224, 20 February 2015.

[30] S. Nakayama, H. Kajiya, K. Okabe and T. Idebe, “Effects of oxidative stress on the expression of 8-oxoguanine and its eliminating enzymes in human keratinocytes and squamous carcinoma cells,” Oral Science International 8 (2011), 11-16. DOI: 10.1016/S1348(11)00004-8

[31] Zhang, Y. Shan and L. Dong, “A comparison of TiO2 and ZnO nanoparticles as photosensitizers in photodynamic therapy for cancer,” J. Biomed Nanotechnology: 2014 Aug; 10(8):1450-7.

## 6. ACKNOWLEDGMENT

This work was supported by the National Institutes of Health / National Institute of Arthritis and Musculoskeletal and Skin Disease, Phase I SBIR, Contract No. 1R43AR067603-01A1. The content is solely the responsibility of the authors and does not necessarily represent the official views of the National Institutes of Health. We are very grateful for this support.